

## Shape Control Simulation on 4-High CVC Mill

WANG Ying-rui<sup>1</sup>, YUAN Jian-guang<sup>1</sup>, LIU Hong-min<sup>2</sup>

(1. Baoshan Iron and Steel Group Co Ltd, Shanghai 200941, China; 2. Yanshan University, Qinhuangdao 066004, China)

**Abstract :** The computation model of shape and crown on 4-high CVC mill was established by combining the stream surface strip element method for analyzing three-dimensional plastic deformation of strip and the influence coefficient method for elastic deformation of rolls, and the simulation of the shape and crown control on 4-high CVC hot strip mill was conducted. The simulated results indicate that the influence of the shifting of CVC work roll on shape and crown is very large, and the shifting of work roll can be used to preset shape and crown. The influence of the bending force of work roll on shape and crown is smaller, and it is suitable to use the bending force of work roll for shape and crown adjustment on line. With the increase of strip width, the exit crown of strip increases firstly and decreases then, and the roll gap becomes smoother increasingly. Meanwhile, the transverse difference of front tension stress decreases firstly and increases then.

**Key words :** 4-high CVC mill; stream surface strip element method; shape; crown; unit rolling pressure; simulation

Shape and profile are the important quality indexes of rolled plate and strip, and shape control is the key technology for plate and strip mills. The research on shape control has an important significance for presetting control of shape and crown and the development of rolling technology. The shape control of wide cold strip rolling on CVC mill was simulated in Ref. [1]. Because the influence of the lateral flow of metal on the form of deformation zone wasn't considered, the three-dimensional plastic deformation of strip and the shape control on CVC cold mill couldn't be analyzed accurately. The shape control model of 4-high hot strip continuous mills was studied in Ref. [2] and Ref. [3]. The influence of the lateral flow of metal on the form of deformation zone wasn't considered either, and the distributions of deformation and stress along the thickness direction of strip were thought to be even, so the three-dimensional plastic deformation of strip couldn't be analyzed accurately, and the accurate shape control model of 4-high hot strip continuous mills couldn't be established. The shape control on 6-high HC and 6-high CVC cold rolling mills was researched in Ref. [4] - Ref. [6] respectively. Due to no consideration of the change in deformation and stress along the thickness direction, they couldn't be used for hot strip rolling or thick plate rolling. The FEM was applied to simulate the process of hot plate continuous rolling in Ref. [7]. Because the rolls were

thought to be rigid, the coupling between the three-dimensional plastic deformation of plate and the elastic deformation of rolls couldn't be realized accurately, and the simulation of the rolling process couldn't be carried out in the actual sense. In this study, the stream surface strip element method<sup>[8]</sup> was employed to accurately analyze the three-dimensional deformations of strip, and the influence coefficient method<sup>[9]</sup> was used to analyze the elastic deformations and thermal deformations of rolls. Moreover, the two methods were combined to construct a mathematical model of shape and crown control on 4-high CVC mill. The simulation of the shape and crown control on 4-high CVC hot steel strip mill was conducted.

### 1 Theoretical Model

#### 1.1 Three-dimensional plastic deformation of plate and strip—stream surface strip element method

The basic assumptions of stream surface strip element method<sup>[8]</sup> are: The rolling process is steady and symmetrical about the plane  $xoy$  (Fig. 1). So, the following analysis and computation consider the upper half above the symmetrical plane  $xoy$  only. The plate (strip) is rigid-plastic in roll gap and elastic outside the roll gap.

The rolling deformation zone shown in Fig. 1, according to the method in Fig. 2, is divided into  $n$

**Foundation item :** Item Sponsored by National Natural Science Foundation of China (50175095, 50374058)

**Biography :** WANG Ying-rui(1974-), Male, Post-doctor; **E-mail :** yingrui\_wang@sina.com; **Revised date :** April 19, 2004

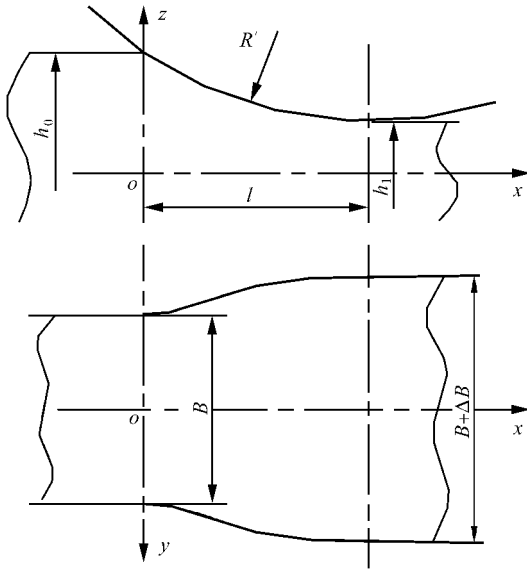


Fig 1 Graphic expression of deformation zone

stream surface (curved surface) strip elements along metal flow direction. In Fig. 1,  $R$  is flattened radius of work roll;  $l$  is length of deformation zone;  $h_0, h_1$  are entry thickness and exit thickness of strip respectively;  $b$  is entry width of strip; and  $b$  is lateral

spread of strip. The ordinates of nodal sections of the strip elements at the entry ( $x=0$ ) are expressed by  $y_i$  ( $i=0, 1, 2, \dots, n$ ), and the ordinates at other place ( $x>0$ ) are unknown. For the convenience of numerical analysis and computation, the stream surface strip elements under the coordinate system  $x-y-z$  are mapped onto the plane strip elements under the coordinate system  $\lambda-\eta$  (the side surfaces and the lower surfaces are planes, and the upper surfaces are cylindrical surfaces), as shown in Fig. 3. In the deformation zone, the lateral displacement function  $W_y(\lambda, \eta)$  and the altitudinal displacement function  $W_z(\lambda, \eta)$  of metal are assumed to be:

$$\begin{aligned} W_y(\lambda, \eta) &= f(\lambda) u_y(\lambda, \eta) \\ W_z(\lambda, \eta) &= g(\lambda) u_z(\lambda, \eta) \end{aligned} \quad (1)$$

From Ref. [10] and Ref. [11], there are:

$$\begin{aligned} f(\lambda) &= 1 + 4 \left[ \frac{\lambda}{l} - 1 \right]^3 + 3 \left[ \frac{\lambda}{l} - 1 \right]^4 \\ g(\lambda) &= 1 - \left[ \frac{\lambda}{l} - 1 \right]^2 \end{aligned} \quad (2)$$

where  $u_y(\lambda, \eta), u_z(\lambda, \eta)$  are lateral and altitudinal displacement functions respectively at the exit of deformation zone ( $x=l$ ).

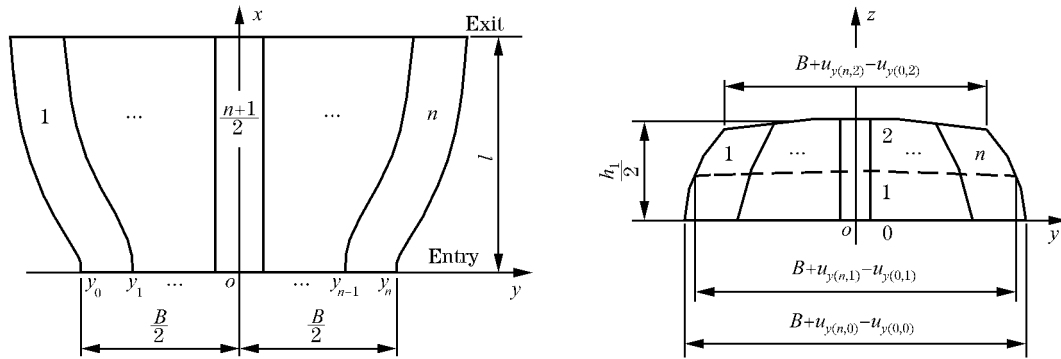


Fig 2 Stream surface strip element division in deformation zone

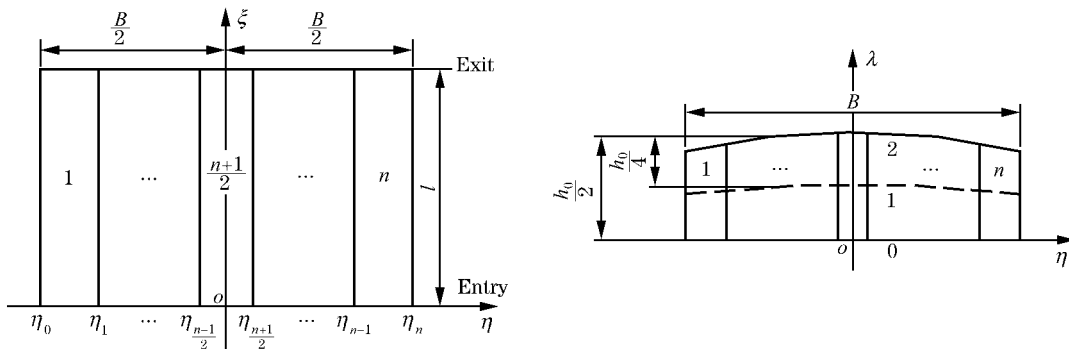


Fig 3 Strip element model in coordinate system

Under the mapping coordinate system, the strip element width  $b_i$  are:

$$b_i = x_i - x_{i-1} = y_i - y_{i-1} \quad (i = 1, 2, \dots, n) \quad (3)$$

$u_y(x, y)$  and  $u_z(x, y)$  are expressed as the third-power spline functions along the lateral direction, assumed to be the quadratic curves along the altitudinal direction, as shown in Fig. 3, and solved by the interpolation method from the displacements on the 0 line, the 1st line and the 2nd line.

Therefore, there are<sup>[8]</sup>:

$$u_y(x, y) = [u_{y(i-1,0)} \phi_1(x) + u_{y(i,0)} \phi_2(x) + u_{y(i-1,1)} \phi_3(x) + u_{y(i,1)} \phi_4(x)] \cdot [u_{y(i-1,2)} \phi_1(x) + u_{y(i,2)} \phi_2(x) + u_{y(i-1,1)} \phi_3(x) + u_{y(i,1)} \phi_4(x)] \quad (4)$$

$$u_z(x, y) = [u_{z(i-1,1)} \phi_1(x) + u_{z(i,1)} \phi_2(x) + u_{z(i-1,1)} \phi_3(x) + u_{z(i,1)} \phi_4(x)] \phi_1(x) + \frac{1}{2} [h_1(x) - h_0(x)] \phi_2(x) \quad (5)$$

where

$$\phi_1(x) = \frac{(x - x_{i-1})^2}{b_i^3} [3b_i - 2(x - x_{i-1})]$$

$$\phi_2(x) = \frac{(x - x_{i-1})^2}{b_i^3} [3b_i - 2(x - x_{i-1})]$$

$$\phi_3(x) = \frac{(x - x_{i-1})^2}{b_i^2} [b_i - (x - x_{i-1})]$$

$$\phi_4(x) = -\frac{(x - x_{i-1})^2}{b_i^2} [b_i - (x - x_{i-1})]$$

$$\phi_0(x) = 1 - 3\left(\frac{x - x_{i-1}}{h_0/2}\right) + 2\left(\frac{x - x_{i-1}}{h_0/2}\right)^2$$

$$\phi_1(x) = 4\left[\frac{x - x_{i-1}}{h_0/2} - \left(\frac{x - x_{i-1}}{h_0/2}\right)^2\right]$$

$$\phi_2(x) = -\frac{x - x_{i-1}}{h_0/2} + 2\left(\frac{x - x_{i-1}}{h_0/2}\right)^2 \quad (6)$$

$u_{y(i, j)} = u_y(x_i, y_j)$ ,  $u_{z(i, 1)} = u_z(x_i, y_1)$ ,  $u_{y(i, j)} = \frac{\partial u_y}{\partial x}(x_i, y_j)$  and  $u_{z(i, 1)} = \frac{\partial u_z}{\partial x}(x_i, y_1)$  ( $i = 0, 1, 2, \dots, n$ ;  $j = 0, 1, 2$ ) are exit lateral and altitudinal displacements and their partial derivatives to  $x$  of the nodal sections respectively;  $\phi_0 = 0$ ,  $\phi_1 = \frac{1}{4} h_0$ ,  $\phi_2 = \frac{1}{2} h_0$ .  $u_y(x, y)$  and  $u_z(x, y)$  satisfy the condition that the first derivatives and the second derivatives of  $u_y$  and  $u_z$  to  $x$  and  $y$  are continuous.  $u_{y(i, j)}$  and  $u_{z(i, 1)}$  ( $i = 0, 1, 2, \dots, n$ ;  $j = 0, 1, 2$ ) are determined by the recurrence method, according to the secondary boundary condition. Therefore, there are  $4(n + 1)$  unknown parameters:  $u_{y(i, j)}$  and  $u_{z(i, 1)}$  ( $i = 0, 1, 2, \dots, n$ ;  $j = 0, 1, 2$ ).

On the above basis, the three-dimensional deformation of plate and strip can be analyzed.

Based on the principle of constant volume and conclusions in Ref. [10] - Ref. [13], the mathematical models of the front tension stress  $\sigma_1(x, y)$  and the back tension stress  $\sigma_0(x, y)$  can be derived as:

$$\sigma_1(x, y) = \bar{\sigma}_1 + \frac{E}{1 - \nu^2} \left[ 1 - \frac{S_1 \left( 1 - \frac{1 - \nu^2}{E} \sigma_{00} \right)}{S_0 \left( 1 + \frac{\partial u_x}{\partial x} \right) \left( 1 + \frac{\partial u_z}{\partial z} \right)} \right] \quad (8)$$

$$\sigma_0(x, y) = \bar{\sigma}_0 + \sigma_{00}(x, y) + \frac{E}{1 - \nu^2} \cdot \left\{ \frac{S_0}{S_n} \left[ \left( 1 + \frac{\partial W_x}{\partial x} \right) \left( 1 + \frac{\partial W_z}{\partial z} \right) \right] - 1 \right\} \quad (9)$$

where  $S_0$ ,  $S_1$  are area of exit cross section and entry cross section respectively;  $S_n$ ,  $x_n$  are area and longitudinal coordinate of neutral plane, respectively;  $\bar{\sigma}_1$ ,  $\bar{\sigma}_0$  are average front and back tension stresses, respectively;  $E$  is elastic modulus of plate (strip);  $\nu$  is Poisson coefficient of plate (strip);  $\sigma_{00}$  is longitudinal residual stress and can be expressed in terms of a polynomial function. When the shape of the entry plate (strip) is good,  $\sigma_{00}(x, y) = 0$ .

From the plastic flow equation of Levy-Mises, the yield condition of Von-Mises and the principle of constant volume, the three-dimensional stress models in the deformation zone are solved.

From the differential equilibrium equations,

$$\frac{\partial \sigma_x}{\partial x} + \frac{\partial \tau_{xy}}{\partial y} + \frac{\partial \tau_{xz}}{\partial z} = 0$$

$$\frac{\partial \tau_{xy}}{\partial x} + \frac{\partial \sigma_y}{\partial y} + \frac{\partial \tau_{yz}}{\partial z} = 0 \quad (10)$$

$$\frac{\partial \tau_{xz}}{\partial x} + \frac{\partial \tau_{yz}}{\partial y} + \frac{\partial \sigma_z}{\partial z} = 0$$

The stress boundary conditions at the entry and the exit of the deformation zone, and the stress boundary condition<sup>[14]</sup> at the interface are:

$$p = -n_x = -(\sigma_x \cos^2 \alpha + \tau_{xy} \cos \alpha \sin \alpha + \tau_{xz} \cos \alpha \sin \alpha) \cos \alpha - (\tau_{xy} \sin \alpha \cos \alpha + \tau_{yz} \sin \alpha \cos \alpha + \sigma_y \sin^2 \alpha) \sin \alpha \quad (11)$$

where  $\sigma_x$ ,  $\sigma_y$ ,  $\sigma_z$ ,  $\tau_{xy}$ ,  $\tau_{yz}$  and  $\tau_{xz}$  are normal stress and shearing stress in the directions  $x$ ,  $y$  and  $z$ , respectively;  $n_x$  is normal stress on the interface;  $\cos \alpha$ ,  $\sin \alpha$  and  $\sin \alpha$  are cosines of the exterior normal of the interface at three directions. The unit rolling pressure  $p$  in the deformation zone can be calculated using a finite difference method.

### 1.2 Elastic deformation of rolls — influence coefficient method

In the range of backup roll body length, the roll body is divided into  $m$  segments with every width of  $y_i$  and central ordinate of  $y_i$  ( $i = 1, 2, 3, \dots, m$ ).

The loading diagram and the segment dividing diagram of rolls are shown in Fig. 4 and Fig. 5. In Fig. 4,  $\delta$  is rightward shifting distance of the upper work roll, and  $\delta > 0$  is for concave roll gap, while  $\delta < 0$  is for convex roll gap.  $p_1(y)$  is unit width rolling pressure;  $q(y)$  is contact pressure between work roll and backup roll;  $F_w$ ,  $F_b$  are bending forces of work roll and backup roll, respectively;  $F_{sl}$ ,  $F_{sr}$  are support-counter forces at left and right press down support points respectively. The coordinate origin of the whole coordinate system is just below the left press support point, namely the altitudinal axis ( $z$  axis) overpasses the left press down support point.

The axis displacements of backup roll and work roll are expressed as:

$$f_{bi} = \sum_{j=1}^m a_{bij} y_j q_j - a_{Fbi} F_b \quad (12)$$

$$f_{wi} = \sum_{j=1}^m a_{wij} y_j (p_{1j} - q_j) - a_{Fwi} F_w + C_1 + \frac{(C_2 - C_1)}{L_w} (y_i - C) \quad (13)$$

The elastic flattening between work roll and backup roll,  $w_{bi}$ , is calculated using the half plane body model, as follows:

$$w_{bi} = i q_i \quad (14)$$

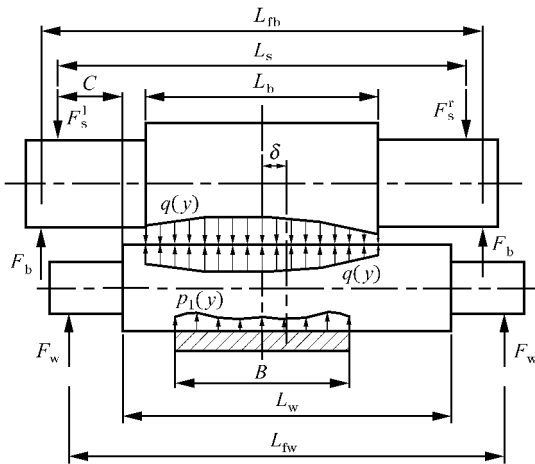


Fig 4 Loading diagram of rolls of 4-high CVC mill

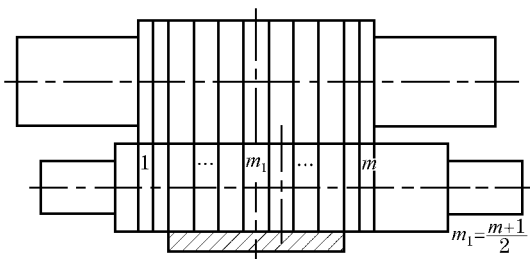


Fig 5 Segment dividing diagram of rolls of 4-high CVC mill

The elastic flattening of work roll between work roll and plate (strip),  $w_i$ , is calculated using the half space body model, as follows:

$$w_i = \sum_{j=1}^m p_{1j} \quad (15)$$

The deformation compatibility equation between work roll and backup roll is:

$$f_{wi} = f_{bi} + w_{bi} + \frac{1}{2} (D_{wi} + D_{bi}) \quad (16)$$

The crown calculation model of work roll is:

$$D_{wi} = D_{w0i} + D_{wti} \quad (17)$$

The thermal crown calculation model of work roll<sup>[12]</sup> is:

$$D_{wti} = D_{wt} \left( \frac{y_i - y_{m_1}}{L_w/2} \right)^2 \quad (18)$$

The transverse distribution of rolled plate (strip) thickness is:

$$h_i = s_0 + f_{wi} + f_{w(m-i)} + w_i + w_{(m-i)} + \frac{1}{2} (D_{wi} + D_{w(m-i)}) + f_{bb}^K \quad (19)$$

where  $i, j$  are subsegment labels of roll,  $i, j = 1, 2, 3, \dots, m$ ;  $a_{wij}$ ,  $a_{bij}$  are deflection influence coefficients of work roll and backup roll respectively, and express the deflection at the point  $y_i$  caused by the unit force acting at the point  $y_j$ ;  $a_{Fwi}$ ,  $a_{Fbi}$  are influence coefficients of bending forces of work roll and backup roll respectively, and express the deflection at the point  $y_i$  caused by the unit bending roll force;  $C_1$ ,  $C_2$  are axis displacements of the left and right end of work roll body respectively;  $C$  is distance between the left press down support point and the left end of work roll body;  $f_w$ ,  $f_b$  are axis deflections of work roll and backup roll respectively;  $w_{wb}$  are flattening coefficient and flattening quantity between work roll and backup roll, respectively;  $w_w$  are flattening coefficient and flattening quantity of work roll between work roll and plate (strip), respectively;  $D_w$ ,  $D_b$  are crowns of work roll and backup roll respectively;  $D_{w0}$ ,  $D_{wt}$  are initial crown and thermal crown of work roll respectively;  $f_{bb}^K$  is rigidity displacement sum of upper and lower work rolls, and depends on the elastic deformation of frame and other loaded parts;  $s_0$  is initial roll gap.

Equations from Eqn. (12) to Eqn. (14) are substituted into Eqn. (16), and the equation group of  $m$  equations is formed. Meanwhile, the equilibrium equations of force and moment of work roll are added again, so the sum of equation is  $(m + 2)$ . In the equation group, there are  $(m + 2)$  unknown numbers  $q_i (i = 1, 2, 3, \dots, m)$ ,  $C_1$  and  $C_2$ , so it can be

solved. Eqn. (15) and Eqn. (16) are substituted into Eqn. (19), and then the thickness of rolled plate (strip) can be solved.

### 1.3 Analysis and computation model of shape and crown for 4-high CVC mill

The analysis and computation flow of shape and crown for 4-high CVC mill is shown in Fig. 6. The three-dimensional plastic deformation analysis of plate (strip) is used to determine the transverse ( $y$  direction) distributions of unit width rolling pressure  $p_1$ , front tension stress  $\sigma_1$ , back tension stress  $\sigma_0$  and so on. The elastic deformation analysis of rolls is used to determine the transverse distribution of unit width contact pressure  $q$  between work roll and backup roll and the loaded roll gap shape  $h_1$  [namely the transverse distribution of the exit plate (strip) thickness]. The above two are coupled, and the exit shape (transverse distribution of  $\sigma_1$ ) and the exit crown of plate (strip) (transverse distribution of  $h_1$ ) under given rolling conditions can be obtained.

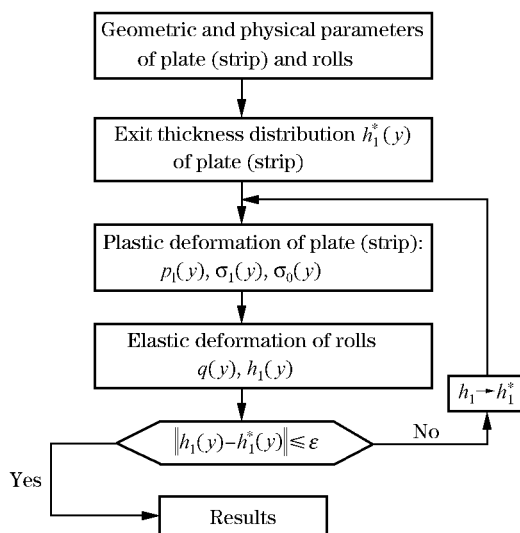


Fig. 6 Flow diagram of analysis and computation of shape and crown

## 2 Simulation Results

Based on the practice on a 4-high CVC hot strip rolling mill, the shape control was studied. The entry width of strip was 1 235 mm. The thickness of strip is 39.214 mm at the entry and 24.477 mm at the exit. The entry yield strength of strip is 100 MPa. The entry crown of strip is 700  $\mu\text{m}$ . The front tension was 186.50 kN, and the back tension is 0

kN. The bending force of work roll was 1 077 kN. The work roll has a diameter of 850 mm and a roll body length of 2 250 mm, and the backup roll has a diameter of 1 500 mm and a roll body length of 2 050 mm. The space between the bending forces of work rolls two ends is 3 150 mm, and the space between the two end press down support points is 3 150 mm. The space between the maximal and minimal diameter of work roll is 1 300 mm. The difference of the maximal and minimal diameter of work roll is 0.599 8 mm. The initial shifting distance ( $\delta_0$ ) of CVC work roll is -10 mm, and the shifting distance ( $\delta$ ) of CVC work roll is -95 mm. The thermal crown of work roll is 350  $\mu\text{m}$ .

### 2.1 Simulation of shape control by work roll shifting

Fig. 7 shows the transverse distribution of exit strip crown ( $h_1$ ) and unit width rolling pressure ( $p_1$ ) under the condition that  $F_w$  is 1 077 kN, and is -75 mm, -25 mm, 25 mm and 75 mm respectively. With the increase of  $\delta$ ,  $h_1$  reduces largely. The transverse change of  $p_1$  becomes more rapidly.

Fig. 8 shows the distribution of  $\sigma_1$  under the condition that  $F_w$  is 1 077 kN, and  $\delta$  is -75 mm, -25 mm, 25 mm and 75 mm respectively. With the increase of  $\delta$ , the transverse difference of  $\sigma_1$  increases from 33 MPa at  $\delta = -75$  mm to 79 MPa at  $\delta = 75$  mm. It is obvious that for thick plate (strip), the larger the change of the proportional crown, the larger the influence on  $\sigma_1$ .

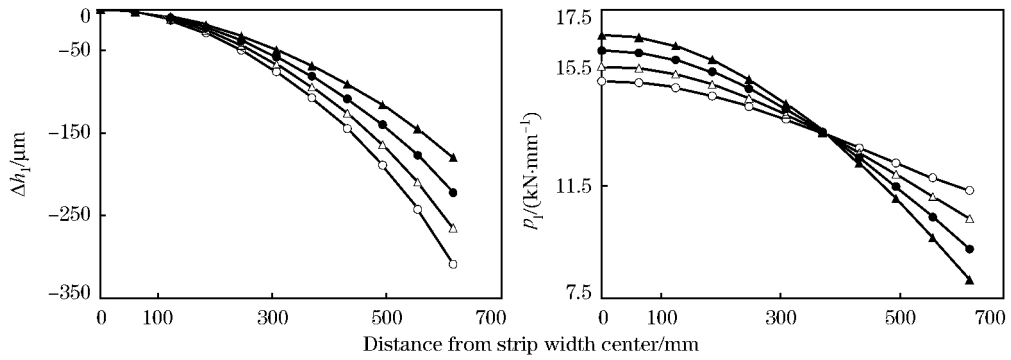
### 2.2 Simulation of bending roll characteristic of work roll

Fig. 9 shows the relation of  $h_1$ ,  $p_1$  and  $F_w$ . With the increase of  $F_w$ ,  $h_1$  changes little, and the transverse change of  $p_1$  increases, but the influence of  $F_w$  is weaker than that of  $\delta$ .

Fig. 10 shows the distribution of  $\sigma_1$  at the exit under the condition that  $\delta$  is -95 mm, and  $F_w$  is 0 kN, 300 kN, 600 kN and 900 kN respectively. With the increase of  $F_w$ , the transverse difference of  $\sigma_1$  increases, in particular at the edges.

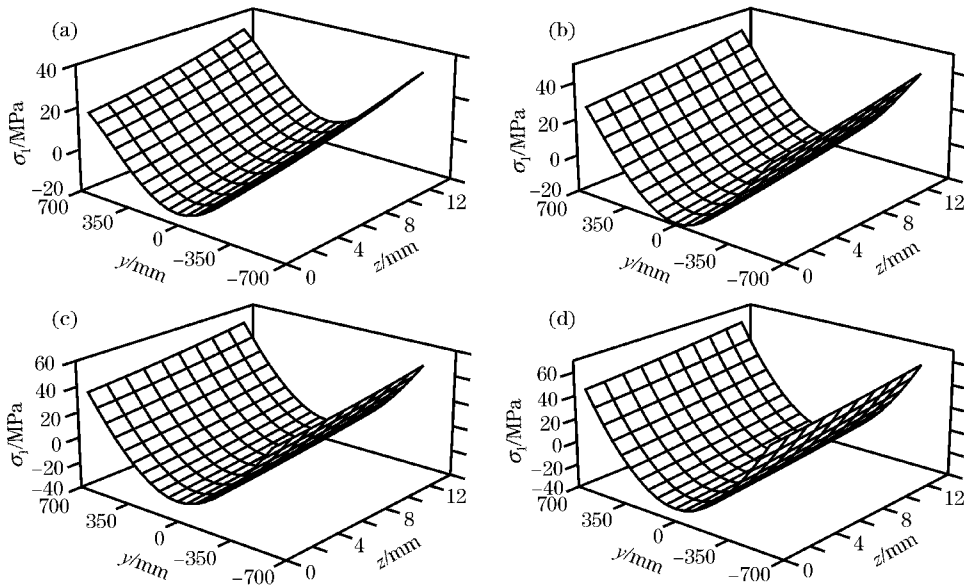
### 2.3 Influence of plate (strip) width on shape and crown

In order to study the influence of plate (strip) width on shape and crown of hot rolled plate (strip) accurately, and to eliminate the influence of other factors, in the simulation, the  $\delta$  was set at 10 mm (namely  $\delta + \delta_0 = 0$ ),  $F_w$  was set at 0 kN, and  $T_1$  was



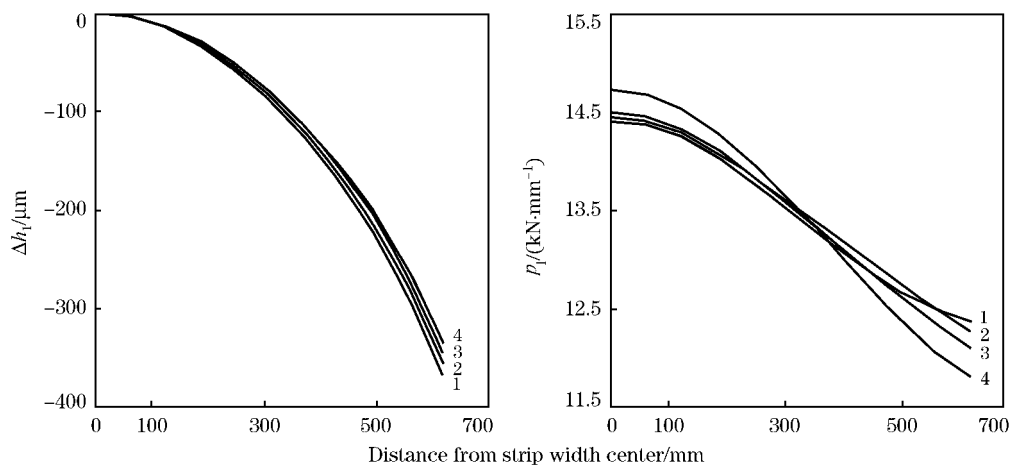
— = - 75 mm; — = - 25 mm; — = 25 mm; — = 75 mm

Fig 7 Influence of on  $h_1$  and  $p_1$  ( $F_w = 1\ 077\ \text{kN}$ )



(a) = - 75 mm; (b) = - 25 mm; (c) = 25 mm; (d) = 75 mm

Fig 8 Influence of on  $\sigma_y$  ( $F_w = 1\ 077\ \text{kN}$ )



1— $F_w = 0\ \text{kN}$ ; 2— $F_w = 300\ \text{kN}$ ; 3— $F_w = 600\ \text{kN}$ ; 4— $F_w = 900\ \text{kN}$

Fig 9 Influence of  $F_w$  on  $h_1$  and  $p_1$  ( $b = 95\ \text{mm}$ )

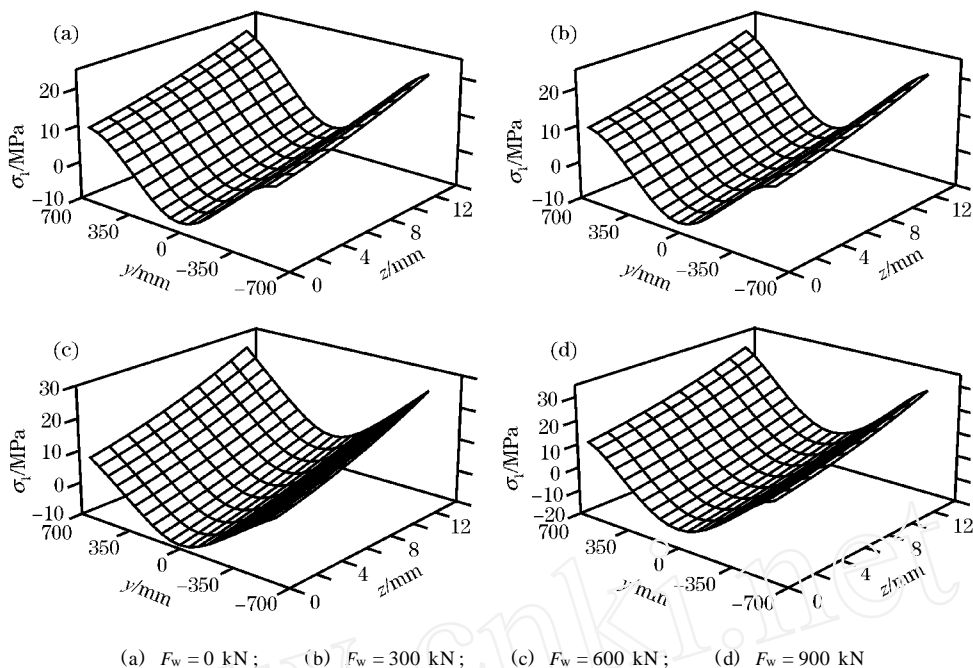


Fig 10 Influence of  $F_w$  on  $\sigma_{x1}$  ( $\delta = -95$  mm)

changed at the same proportion as the plate (strip) width.

Fig. 11 shows the distributions of  $h_1$  and  $p_1$  for different  $B$ . With the increase of  $B$ ,  $h_1$  increases firstly and decreases then, and  $h_1$  ( $=274.335 \mu\text{m}$ ) at  $B = 1635$  mm is already slightly less than  $h_1$  ( $=274.388 \mu\text{m}$ ) at  $B = 1435$  mm. Meanwhile, the distribution of roll gap becomes smoother increasingly. In addition, with the increase of  $B$ , the transverse difference of  $p_1$  decreases firstly and increases then. The reason can be that  $h_1$  increases firstly and decreases then, and the action width of the  $y$ -direction friction stress ( $\sigma_y$ ) increases with the increase of  $B$ , making the transverse change of  $\sigma_1$  increase.

Fig. 12 shows the distribution of  $\sigma_1$  under different  $B$ . With the increase of  $B$ , the transverse difference of  $\sigma_1$  decreases firstly and increases then, however, the altitudinal change of  $\sigma_1$  is very small, which may be that the strip width/thickness ratio is already very large, and even the strip width/thickness ratio increases continuously again, the altitudinal changes of stresses and deformations of plate (strip) may be not obvious.

### 3 Conclusions

(1) With the increase of  $\delta$ ,  $h_1$  reduces largely, and the transverse difference of  $\sigma_1$  increases. With increasing  $F_w$ ,  $h_1$  reduces lightly, and the transverse difference of  $\sigma_1$  increases, in particular at

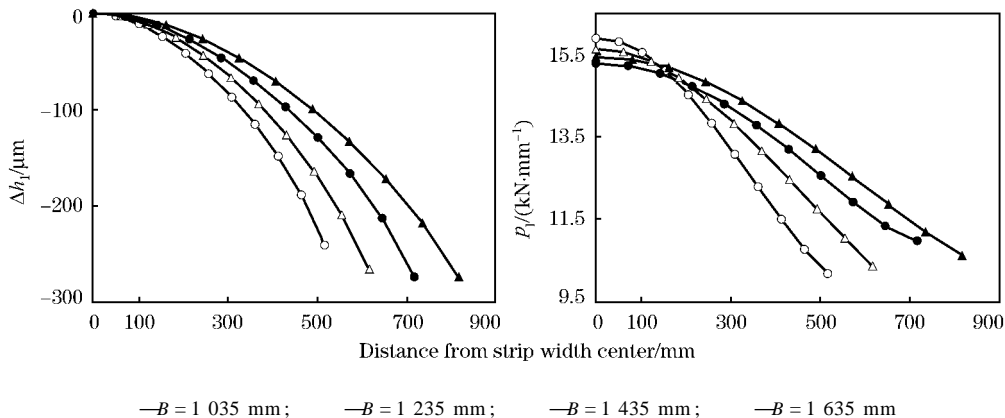


Fig 11 Influence of  $B$  on  $h_1$  and  $p_1$  ( $\delta = 10$  mm,  $F_w = 0$  kN)

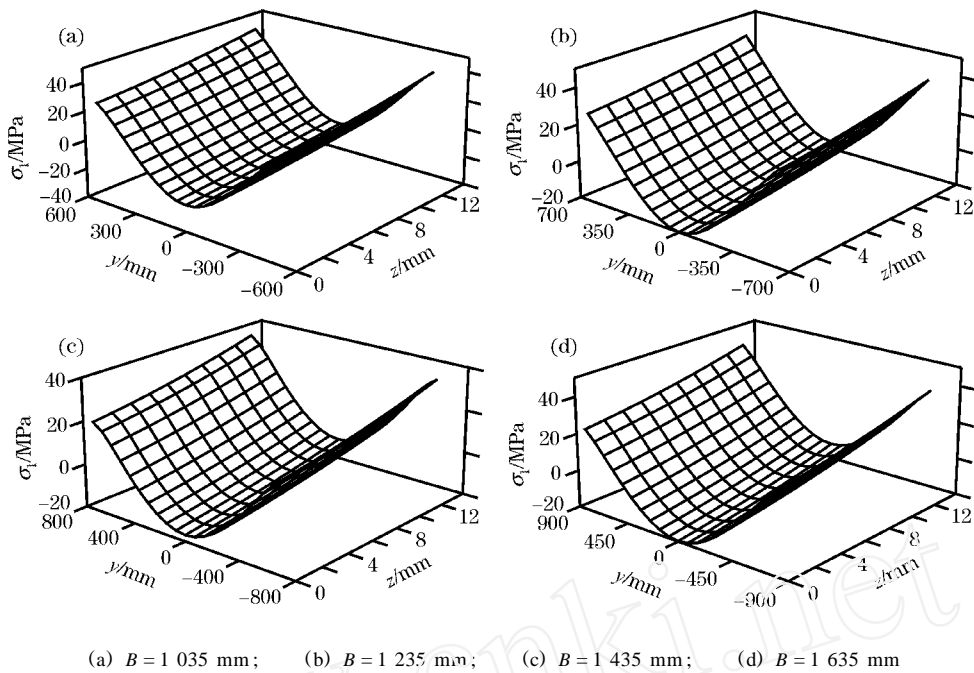


Fig 12 Influence of B on  $\sigma_x$  ( $h = 10 \text{ mm}$ ,  $F_w = 0 \text{ kN}$ )

the edges. With the increase of  $B$ ,  $h_1$  increases firstly and decreases then, and meanwhile, the roll gap becomes smoother increasingly, and the transverse difference of  $\sigma_x$  decreases firstly and increases then.

(2) The influence of  $\sigma_x$  on shape and crown is very large, and it is suitable for shape and crown preset. The influence of  $F_w$  on shape and crown is smaller, and it is suitable for the on-line adjustment of shape and crown.

**References :**

[1] WANG Hong-xu, LIU Hong-min. Simulation on Characteristics of Profile Control in Cold Wide Strip Rolling on CVC Mill [J]. Research on Iron and Steel, 1997, (2) : 21-23, 54 (in Chinese).

[2] LIU Hong-min, Sanfilippo F, Dolici F. Flatness Control Mathematic Model of Hot Steel Strip Continuous Rolling Mill [J]. Iron and Steel, 1996, 31(10) : 30-34 (in Chinese).

[3] GUO Jiar-bo. Research on Shape and Profile Control Technology of Hot Steel Strip Continuous Mills [D]. Qinhuangdao : Yanshan University, 1998 (in Chinese).

[4] PENG Yan, ZHENG Zhen-zhong, LIU Hong-min. Simulation Research of Cold Rolled Strip Shape Control in 6-Roller HC Mill [J]. China Mechanical Engineering, 2000, 11(9) : 1061-1063 (in Chinese).

[5] LIU Hong-min, ZHENG Zhen-zhong, PENG Yan, et al. Computer Simulation of the Roll Contact Pressure Characteristic for 6-High CVC Wide Strip Mill [J]. Chinese Journal of Mechanical Engineering, 2000, 36(8) : 69-73 (in Chinese).

[6] LIU Hong-min, ZHENG Zhen-zhong, PENG Yan. Computer Simulation of Shape Control Character of 6-High CVC Wide Strip Mill [J]. Journal of Iron and Steel Research, 2001, 13 (1) : 14-18 (in Chinese).

[7] DU Feng-shan, ZHOU Wei-hai, ZANG Xin-liang. Computer Simulation of Hot Continuous Rolling Process of Plate [J]. Chinese Journal of Mechanical Engineering, 2001, 37(12) : 67-69 (in Chinese).

[8] LIU Hong-min, WANG Ying-rui. Stream Surface Strip Element Method for Simulation of the Three-Dimensional Deformations of Plate and Strip [J]. Chinese Journal of Mechanical Engineering, 2003, 39(7) : 94-100 (in Chinese).

[9] WANG Ying-rui, JIANG Guang-biao, LIU Hong-min. Complete Mill Simulation of the Rolling Process of 4-High Hot Steel Strip Continuous Mills Based on the Stream Surface Strip [J]. China Mechanical Engineering, 2003, 14(21) : 1853-1856 (in Chinese).

[10] LIU Hong-min, ZHENG Zhen-zhong, PENG Yan. Streamline Strip Element Method for Analysis of the Three-Dimensional Stresses and Deformations of Strip Rolling [J]. International Journal for Numerical Methods in Engineering, 2001, 50(5) : 1059-1076.

[11] LIU Hong-min, LIAN Jia-chuang, PENG Yan. Third-Power Spline Function Strip Element Method and Its Simulation of the Three-Dimensional Stresses and Deformations of Cold Strip Rolling [J]. Journal of Materials Processing Technology, 2001, 116(2-3) : 235-243.

[12] LIU Hong-min. Three-Dimensional Rolling Theory and Its Applications [M]. Beijing : Science Press, 1999 (in Chinese).

[13] LIU Hong-min, LIAN Jia-chang. Linear Strip Element Method for Analyzing Lateral Flow of Metal and Transverse Distributions of Tension Stresses of Cold Rolled Strip [J]. Journal of Iron and Steel Research, 1992, 4(3) : 37-44 (in Chinese).

[14] WANG Ying-rui, LIU Hong-min. Simulation Research on the Rolling Force of Hot Steel Strip Rolling under Accurate Contact Boundary Condition [J]. Journal of Iron and Steel Research, 2004, 16(1) : 34-39 (in Chinese).